nature structural & molecular biology

T-cell receptor recognition of HLA-DQ2–gliadin complexes associated with celiac disease

Jan Petersen[1,8], Veronica Montserrat[2,8], Jorge R Mujico[2], Khai Lee Loh[1], Dennis X Beringer[1], Menno van Lummel[2], Allan Thompson[2], M Luisa Mearin[3], Joachim Schweizer[3], Yvonne Kooy-Winkelaar[2], Jeroen van Bergen[2], Jan W Drijfhout[2], Wan-Ting Kan[4], Nicole L La Gruta[4], Robert P Anderson[5], Hugh H Reid[1,9], Frits Koning[2,9] & Jamie Rossjohn[1,6,7,9]

Celiac disease is a T cell–mediated disease induced by dietary gluten, a component of which is gliadin. 95% of individuals with celiac disease carry the *HLA* (human leukocyte antigen)-*DQ2* locus. Here we determined the T-cell receptor (TCR) usage and fine specificity of patient-derived T-cell clones specific for two epitopes from wheat gliadin, DQ2.5-glia-α1a and DQ2.5-glia-α2. We determined the ternary structures of four distinct biased TCRs specific for those epitopes. All three TCRs specific for DQ2.5-glia-α2 docked centrally above HLA-DQ2, which together with mutagenesis and affinity measurements provided a basis for the biased TCR usage. A non–germline encoded arginine residue within the CDR3β loop acted as the lynchpin within this common docking footprint. Although the TCRs specific for DQ2.5-glia-α1a and DQ2.5-glia-α2 docked similarly, their interactions with the respective gliadin determinants differed markedly, thereby providing a basis for epitope specificity.

Celiac disease (CD) is a T cell–mediated inflammatory disorder of the small intestine that affects approximately 1% of the population in westernized countries[1–3]. CD is triggered by gluten ingestion, with gluten-specific CD4$^+$ T cells typically being found in patients with CD; the presence of such cells within the lamina propria has been associated with small intestine tissue damage. CD is linked strongly to the HLA locus, specifically *HLA-DQ2* (*A1*0501–B1*0201*) and/or *HLA-DQ8* (*A1*0301–B1*0302*)[1,4–6]. *HLA-DQ8*$^+$ *HLA-DQ2*$^-$ individuals represent approximately 5% of patients with CD[7]. In stark contrast, approximately 95% of patients with CD are *HLA-DQ2*$^+$, and thus HLA-DQ2–mediated CD is a much more substantial problem clinically than HLA-DQ8–mediated CD[7].

Regardless of genetic associations, the only available treatment for CD is strict adherence to a lifelong gluten-free diet[3]. To compound matters, disease onset, severity and sensitivity toward gluten intake are highly variable among patients with CD[3]. Although it is clear that the risk of CD development is strongly dependent on the *HLA-DQ* genotype, the molecular basis for the highly variable disease outcome is unknown, and it is not understood how the T-cell response in the lamina propria leads to inflammation in the epithelium.

Both HLA-DQ8– and HLA-DQ2–mediated CD require tissue transglutaminase–mediated deamidation (conversion of glutamine residues to glutamate) of gluten epitopes[8]. The deamidation of gluten epitopes generally engenders higher-avidity binding to HLA-DQ8 and HLA-DQ2 molecules and stronger T-cell responses toward gluten peptides, and this is likely a crucial step toward CD pathogenesis[9–12]. Nevertheless, the extent, pattern and molecular basis of the deamidation dependence can differ between these forms of CD. For example, whereas HLA-DQ8–restricted gluten peptides can require deamidation at the P1 and/or P9 positions[9,12–15], HLA-DQ2–restricted gluten determinants are frequently dependent on deamidation of a single glutamine at P4 or P6 for optimal T-cell reactivity[16–19].

In HLA-DQ2–associated CD, a series of gluten epitopes have been characterized, including peptides derived from wheat gluten subfractions (α-, β-, γ- and ω-gliadin and low- and high-molecular-weight glutenins) and closely related sequences in barley hordeins and rye secalins. The immunodominant wheat gluten peptide comprises two overlapping T-cell determinants (DQ2.5-glia-α1a (PFPQPELPY) and DQ2.5-glia-α2 (PQPELPYPQ)) contained within a single, protease-resistant α-gliadin 11-mer[16,20]. Structural studies showed how a hydrogen-bonding network enhances the binding of the deamidated gliadin determinant, DQ2.5-glia-α1a, to HLA-DQ2 (ref. 10). However, the basis of the deamidation dependence of the other HLA-DQ2–restricted epitopes, including the DQ2.5-glia-α2 epitope, is unknown[21]. Notably, T cells specific for the wheat α-gliadin 11-mer contribute only partially to the immunogenicity of rye or barley. Here, T cells specific for the related wheat ω-gliadin 11-mer encompassing two other epitopes (DQ2.5-glia-ω1 and DQ2.5-glia-ω2) contribute most

[1]Department of Biochemistry and Molecular Biology, School of Biomedical Sciences, Monash University, Clayton, Victoria, Australia. [2]Department of Immunohematology and Blood Transfusion, Leiden University Medical Center, Leiden, The Netherlands. [3]Department of Pediatrics, Leiden University Medical Center, Leiden, The Netherlands. [4]Department of Microbiology and Immunology, Peter Doherty Institute for Infection and Immunity, University of Melbourne, Parkville, Victoria, Australia. [5]ImmusanT, Inc., Cambridge, Massachusetts, USA. [6]Institute of Infection and Immunity, Cardiff University School of Medicine, Heath Park, Cardiff, UK. [7]Australian Research Council Centre of Excellence in Advanced Molecular Imaging, Monash University, Clayton, Victoria, Australia. [8]These authors contributed equally to this work. [9]These authors jointly directed this work. Correspondence should be addressed to H.H.R. (hugh.reid@monash.edu), F.K. (f.koning@lumc.nl) or J.R. (jamie.rossjohn@monash.edu).

Received 12 February; accepted 28 March; published online 28 April 2014; doi:10.1038/nsmb.2817

Table 1 HLA-DQ2.5–restricted T-cell clones and their TCR gene usage

DQ2.5-glia-α1[a]	TRAV	TRAJ	CDR3α	TRBV	TRBJ	TRBD	CDR3β
N10	TRAV38-2/DV8*01	47*01	CAYRSGYMEYGNKLV	29-1*01	2-3*01	1*01	CSVSGGPSTDTQYF
L3-14	4*01	20*01	CLVGDNDYKLSF	29-1*01	1-6*02	1*01	CSVGQTDSPLHF
N12	22*01	24*01	CAVELGDSWGKFQF	29-1*01	2-2*01	1*01	CSAGQGGTGELFF
G1	36/DV7*01	32*01	CAAPGGATNKLIF	29-1*01	2-5*01	2*02	CSVAALAGFQETQYF
L10	8-3*01	44*01	CAVGWEDGTASKLTF	20-1*01	2-3*01	2*02	CSASRWRSTDTQYF
S2	4*01	4*01	CLVGDGGSFSGGYNKLIF	20-1*01	2-5*01	2*01	CSAGVGGQETQYF
L5-105	20*01	37*01	CAVQADGNTGKLIF	20-1*01	2-5*01	1*01	CSAYRTWDQETQYF
L5-109	24*01	53*01	CAFIGGSNYKLTF	20-1*01	2-2*01	1*01	CSAREPDNTGELFF
L5-104	ND		ND	20-1*01	2-7*01	2*01	CSARGYGLANPYEQY
N13	35*01	34*01	CAGPYNTDKLIF	7-6*01	2-3*01	2*02	CASSLASAGGTDTQYF
H49	29/DV5*01	32*01	CAASANYGGATNKLIF	7-3*01	1-1*01	1*01	CASSLNWDTEAFF
L6	21*01	21*01	CAVTLGGGSEKLVF	5-5*01	1-1*01	1*01	CASSFSPAGSEAFF
LS2.8/3.15	8-3*01	33*01	CAVGAGSNYQLIW	5-5*01	2-1*01	-	CASSLEGQGASEQFF
S3	4*01	4*01	CLVAGAGGYNKLIF	4-2*01	2-5*01	2*01	CASSQGLAGVQETQYF
N14	35*01	32*01	CAGPSGATNKLIF	5-6*01	2-3*01	2*01	CASSPTALGTDTQYF
DQ2.5–glia-α2							
D2	26-1*01	45*01	CIVLGGADGLTF	7-2*01	2-3*01	2*01	CASSFRFTDTQYF
S16	26-1*01	32*01	CIVWGGATNKLIF	7-2*01	2-3*01		CASSVRSTDTQYF
JR5.1	26-1*01	54*01	CIAFQGAQKLVF	7-2*01	2-3*01	2*01	CASSFRALAADTQYF
S4	4*01	17*01	CLVGEAAGNKLTF	7-2*01	2-7*01	2*01	CASSIRTSGDHEQYF
D1	8-3*01	42*01	CAVGRGGSQGNLIF	4-2*01	2-1*01	1*01	CASSQYQSLVRGNNEQFF
N4	14/DV4*01	28*01	CAMREGRGAGSYQLTF	4-2*01	2-3*01	1*01	CASSFPQVTDTQYF
L3-13	14/DV4*03	40*01	CAMSVLSGTYKYIF	4-1*01	2-5*01	1*01	CASSHVDRGGETQYF

[a]DQ2 epitope nomenclature according to Sollid *et al.*[41]. ND, not determined.

to the immunogenicity of barley and rye[22,23]. T cells recognizing two further deamidated peptides, one unique to barley hordein (including the determinant DQ2.5-Hor-1) and the other to rye secalin (including the determinant DQ2.5-Sec-1), also make marked contributions to the immunogenicity of barley and rye, respectively. Notably, most T-cell reactivity in HLA-DQ2.5–associated CD is directed toward three highly homologous peptides (encompassing DQ2.5-glia-α1, DQ2.5-glia-α2, DQ2.5-ω1, DQ2.5-ω2 and DQ2.5-Hor-1) whose relative importance depends on whether wheat, barley or rye is ingested[24].

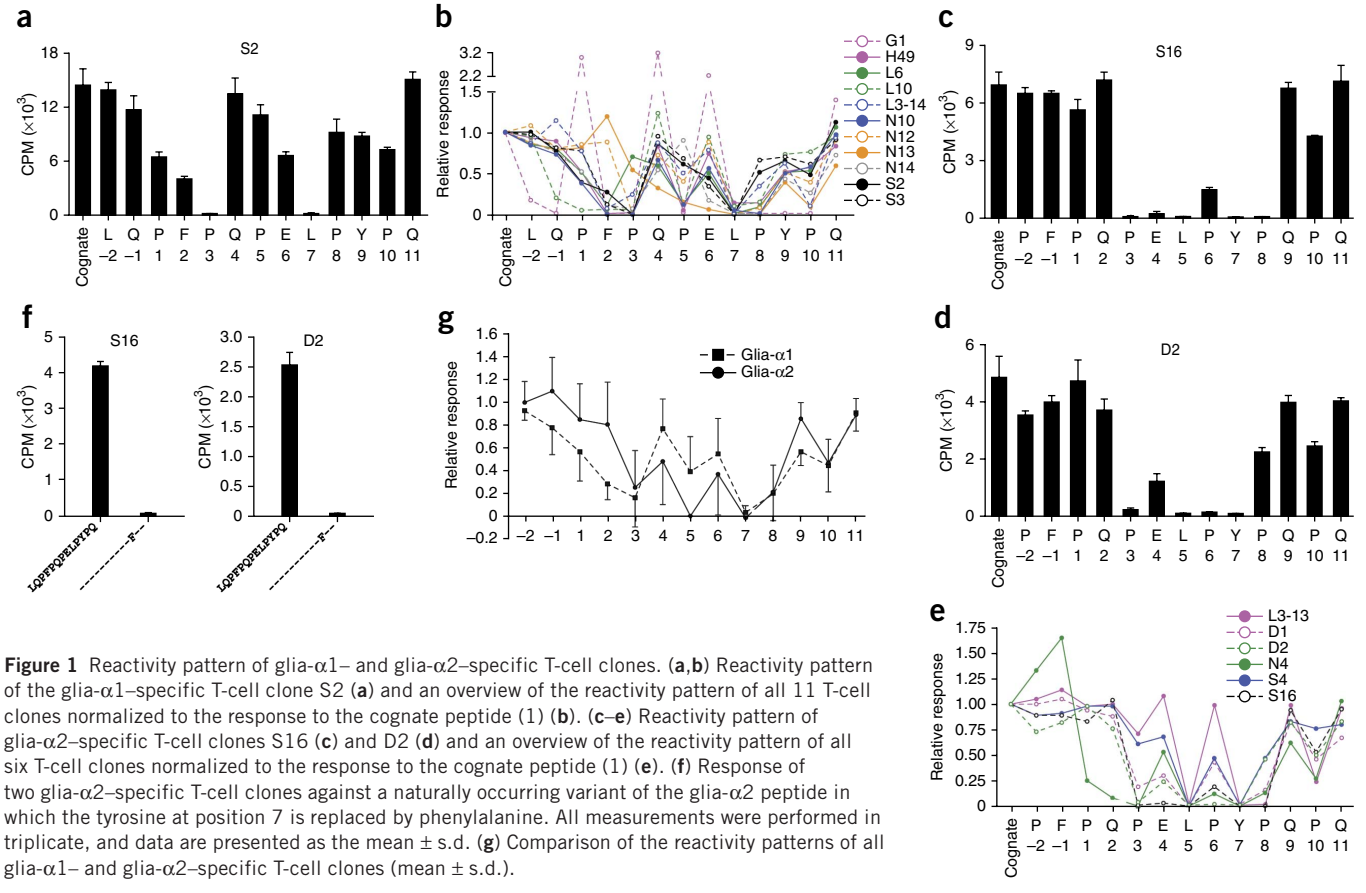

Figure 1 Reactivity pattern of glia-α1– and glia-α2–specific T-cell clones. (**a**,**b**) Reactivity pattern of the glia-α1–specific T-cell clone S2 (**a**) and an overview of the reactivity pattern of all 11 T-cell clones normalized to the response to the cognate peptide (1) (**b**). (**c**–**e**) Reactivity pattern of glia-α2–specific T-cell clones S16 (**c**) and D2 (**d**) and an overview of the reactivity pattern of all six T-cell clones normalized to the response to the cognate peptide (1) (**e**). (**f**) Response of two glia-α2–specific T-cell clones against a naturally occurring variant of the glia-α2 peptide in which the tyrosine at position 7 is replaced by phenylalanine. All measurements were performed in triplicate, and data are presented as the mean ± s.d. (**g**) Comparison of the reactivity patterns of all glia-α1– and glia-α2–specific T-cell clones (mean ± s.d.).

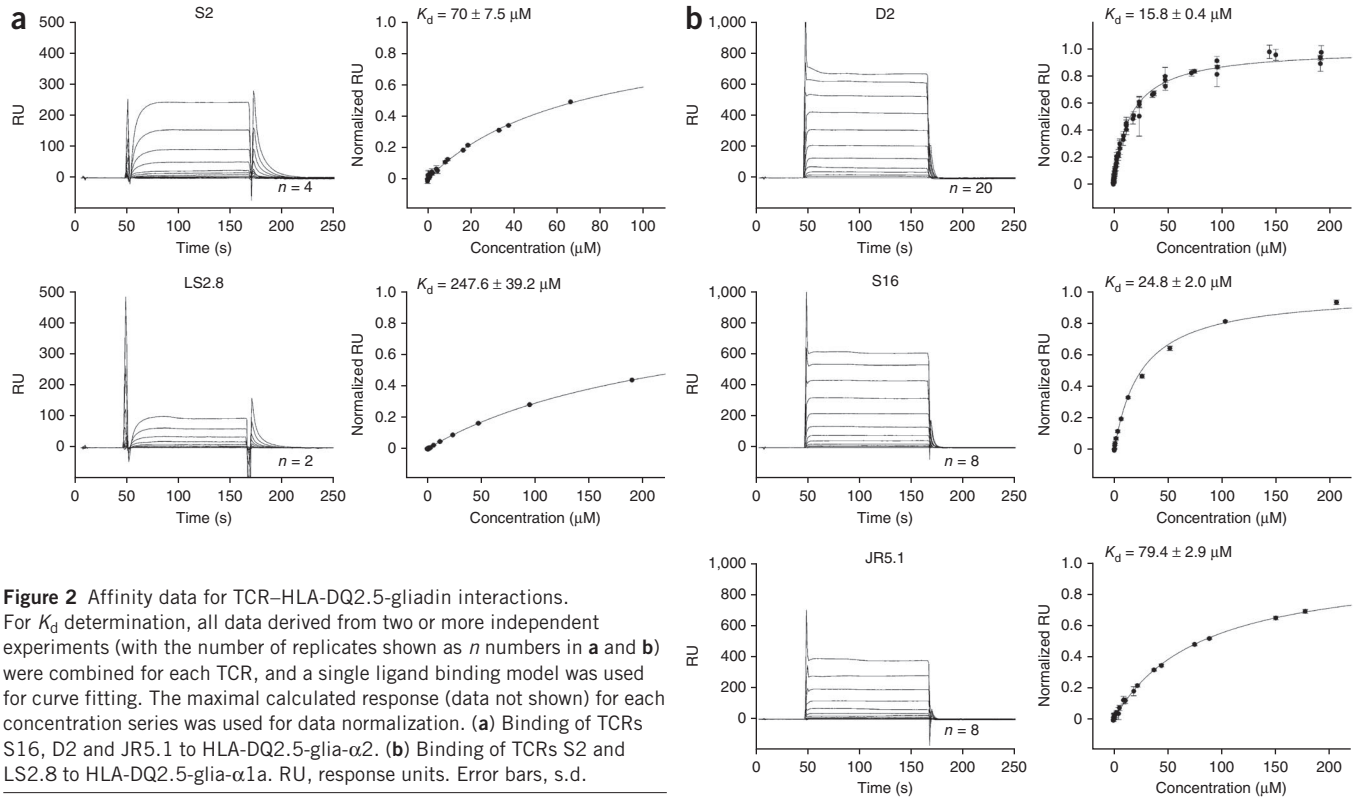

Figure 2 Affinity data for TCR–HLA-DQ2.5-gliadin interactions. For K_d determination, all data derived from two or more independent experiments (with the number of replicates shown as *n* numbers in **a** and **b**) were combined for each TCR, and a single ligand binding model was used for curve fitting. The maximal calculated response (data not shown) for each concentration series was used for data normalization. (**a**) Binding of TCRs S16, D2 and JR5.1 to HLA-DQ2.5-glia-α2. (**b**) Binding of TCRs S2 and LS2.8 to HLA-DQ2.5-glia-α1a. RU, response units. Error bars, s.d.

Our understanding of the role of gluten epitopes in HLA-DQ8–mediated CD is growing[9]. For example, it was recently established that the T-cell response to HLA-DQ8-glia-α1 was characterized by biased *TRBV9*01* gene usage[25]. Whereas an average of 2% of CD4$^+$ T cells isolated from peripheral blood mononuclear cells (PBMCs) expressed *TRBV9*01*, an average of 15% of cells in mixed T-cell lines isolated from biopsies of four patients with CD expressed this gene[25]. The elevated proportion of CD4$^+$ T cells expressing TRBV9*01 in gluten-reactive T-cell lines from biopsies of patients with CD correlated with DQ8-glia-α1 reactivity. Therefore, biased *TRBV9*01* usage appeared to be a main characteristic of the T-cell response to the DQ8-glia-α1 determinant. The structure of a TRBV9*01$^+$ TCR bound to HLA-DQ8-glia-α1 provided a basis for understanding the specificity requirements toward the α1-gliadin determinant and the basis of the *TRBV9*01* bias[25]. Our understanding of HLA-DQ2–mediated CD is less clear, even though this form of the disease is much more prevalent. Nevertheless, it was recently demonstrated that the HLA-DQ2.5-glia-α2–specific T-cell response is dominated by T cells expressing *TRAV26-1* and *TRBV7-2*, although the molecular basis for this biased gene usage remains unknown[26–28]. Moreover, a highly conserved, non–germline encoded arginine residue within the complementarity-determining region (CDR) 3β loop within the DQ2.5-glia-α2–responding T-cell repertoire has been noted[27], although the basis of this conservation was also unclear.

Given the strong association of the *HLA-DQ2* locus in CD and the central role T cells have in this disease, we sought to gain a greater understanding of the molecular basis governing the TCR–HLA-DQ2–gliadin axis. In conjunction with functional, mutagenesis and affinity measurements, we determined the structures of three TRAV26-1–TRBV7-2$^+$ TCR–HLA-DQ2.5-glia-α2 complexes and compared them to a TRAV4*01–TRBV20-1*01$^+$ TCR–HLA-DQ2.5-glia-α1 a complex. We provide detailed insight into how the adaptive immune system responds to two DQ2-restricted immunodominant gliadin determinants derived from wheat.

RESULTS

TCR usage against DQ2.5-glia-α1a and DQ2.5-glia-α2

To investigate the responding T-cell repertoire to the DQ2.5-glia-α1a and DQ2.5-glia-α2 epitopes, we isolated 15 T-cell clones from intestinal biopsies of 7 patients with CD specific for glia-α1 and 7 T-cell clones isolated from 5 patients specific for glia-α2 and determined their TCR usage. All T-cell clones expressed a unique TCR, indicating that they are independently derived (**Table 1**).

The HLA-DQ2.5-glia-α1–restricted TCRs showed TRBV selection bias[29,30] in that 9 out of 15 clones used *TRBV20-1*01* or *TRBV29-1*01*, which are two TRBV genes that cluster together. Moreover, three clones (L3-14, S2 and S3) used the *TRAV4*01* gene (**Table 1**). No bias involving both *TRAV* and *TRBV* genes was evident, and there were not any consistent motifs encoded by their respective CDR3α and CDR3β loops (**Table 1**). In contrast and in agreement with previous observations[26,27], four (D2, S4, S16 and JR5.1) of the HLA-DQ2.5-glia-α2–restricted T-cell clones displayed biased *TRBV7-2* gene usage, and three (D2, S16 and JR5.1) of these used *TRAV26-1* with conserved motifs encoded within their respective CDR3 loops (**Table 1**). Clone S4 is distinguished by the *TRAV4*01* gene (**Table 1**). Furthermore, the CDR3β loop of all the *TRBV7-2*$^+$ TCRs contains an arginine at position 5, two clones (D2 and S16) exhibited an ASSXRXTDTQY motif[26,27] (**Table 1**), and we observed biased selection of the *TRAJ2*01* gene segment in all four clones. Two *TRBV7-2*$^+$ clones, JR5.1 and S4, possessed slightly longer CDR3β loops with two extra residues compared to the motif described above[26,27]. Accordingly, we observed a greater degree of biased TCR usage against the glia-α2 determinant in comparison to the glia-α1 peptide.

Fine specificity toward gliadin determinants

To determine the fine specificity of a panel of individual T-cell clones, we measured their proliferative response toward variants of their cognate antigen in which we systematically replaced each of the amino acids with alanine. Peptide-binding assays showed that the substitutions did not have a major impact on HLA-DQ2 binding affinity, with the exception of replacement of P6 glutamic acid in the DQ2.5-glia-α1a peptide (data not shown), which was previously shown to be the main anchor residue in this peptide[10].

For DQ2.5-glia-α1a, substitutions in and outside the nine-amino-acid core affected T-cell recognition of the peptide by individual T-cell clones in a T cell clone–dependent manner (**Fig. 1a** shows clone S2 and **Fig. 1b** shows an overview of the panel of clones). Alanine substitutions at the P3 and P7 positions abrogated the response of clone S2, whereas substitutions at P2 had less impact. Similarly, for the other T-cell clones, the impact of alanine substitutions at P1, P2 and P6 varied from enhanced T-cell responses to almost complete abrogation of the T-cell response (**Fig. 1b**). Also, we observed large variation with substitutions at P4, P5 and P8 in the nine-amino-acid core of the peptide. In contrast, the P7 leucine to alanine substitution abolished antigen recognition by all T-cell clones, indicating that this amino acid is critical for recognition of DQ2.5-glia-α1a (**Fig. 1a**,**b**).

Next we analyzed the impact of alanine substitutions on the reactivity of six DQ2.5-glia-α2–specific T-cell clones (**Fig. 1c**,**d**). The effect of the alanine substitutions was also T cell–clone dependent. For example, for the T-cell clones S16 and D2, alanine substitutions at P3 through P7 largely abolished T-cell reactivity (**Fig. 1c**,**d**), whereas such substitutions had less effect on the other T-cell clones (**Fig. 1e**). Notably, alanine substitution at either P5 leucine or P7 tyrosine abrogated the response of all DQ2.5-glia-α2–specific T-cell clones, pointing to a critical role of the amino acids at these positions (**Fig. 1c–e**). Indeed, the P7 tyrosine is particularly critical, as even the relatively conservative substitution of tyrosine by phenylalanine at P7 abrogated recognition in the glia-α2–specific T-cell clones tested (**Fig. 1f**). Overall, the impacts of the alanine substitutions on the reactivities of the glia-α1– and glia-α2–specific T-cell clones were remarkably similar (**Fig. 1g**).

Affinity measurements

Next we expressed, refolded and purified the HLA-DQ2.5-glia-α1a–restricted TCRs (S2 and LS2.8) and the HLA-DQ2.5-glia-α2–restricted TCRs (S16, D2 and JR5.1) (data not shown) and measured their steady-state affinities (K_d) for the peptides using surface plasmon resonance (SPR) analysis (**Fig. 2a**,**b**). Neither the S2 nor the LS2.8 TCR for HLA-DQ2.5-glia-α1a showed any appreciable affinity toward HLA-DQ2.5-glia-α2 (data not shown), thereby highlighting the lack of cross-reactivity between these epitope-specific TCRs.

The affinity values of the S16, D2 and JR5.1 TCRs toward HLA-DQ2.5-glia-α2 were, on average, lower than the affinity values observed when TRBV9-1$^+$ TCRs interacted with HLA-DQ8-glia-α1 (average ~6.5 μM, range 1–11 μM)[25]. Nevertheless, the affinity values for some of the HLA-DQ2–restricted TCRs were more in line with the affinity values often observed for microbial or non-self TCR–pMHC-II interactions (~30 μM)[31], whereas the LS2.8 and JR5.1 TCRs exhibited affinity values that were in the range typically associated with the low-affinity autoreactive TCR–pMHC complexes (~100–200 μM)[32,33]. Notably, the JR5.1 TCR exhibited much weaker affinity toward HLA-DQ2.5-glia-α2 than did the S16 and D2 TCRs despite these three TCRs sharing the same Vα and Vβ domains. This observation indicates that CDR3 variability can have a marked impact on the affinity of the interaction toward HLA-DQ2.5-glia-α2.

Table 2 Data collection and refinement statistics

	S2 TCR HLA-DQ2.5-glia-α1a	S16 TCR HLA-DQ2.5-glia-α2	D2 TCR HLA-DQ2.5-glia-α2	JR5.1 TCR HLA-DQ2.5-glia-α2
Data collection				
Space group	*C*121	*C*121	*C*121	*C*121
Cell dimensions				
a, *b*, *c* (Å)	233.027, 142.239, 101.09	261.569, 57.87, 137.411	266.024, 60.266, 138.235	130.93, 84.84, 109.68
α, β, γ (°)	90, 109.79, 90	90, 114.05, 90	90, 114.04, 90	90, 92.99, 90
Resolution (Å)	46.85–3.2	40.99–2.8	43.48–3.0	60.47–2.7
R_{merge}	0.1593 (0.5541)	0.04927 (0.4334)	0.07389 (0.5649)	0.1061 (0.4744)
I / σI	4.24 (1.51)	13.82 (1.90)	8.10 (1.46)	5.87 (1.61)
Completeness (%)	96.06 (97.15)	93.22 (69.33)	96.48 (98.05)	97.77 (87.01)
Redundancy	1.9 (1.8)	2.0 (1.8)	1.9 (1.9)	1.9 (1.8)
Refinement				
Resolution (Å)	46.85–3.2 (3.314–3.2)	40.99–2.8 (2.901–2.801)	43.48–3.0 (3.107–3.0)	60.47–2.7 (2.797–2.7)
Number of reflections	49,208 (4,949)	43,694 (3,230)	39,263 (3,930)	32,383 (2,846)
R_{work} / R_{free}	0. 2058 / 0.2395 (0.2351 / 0.2879)	0.2231 / 0.2385 (0.2527 / 0.2709)	0.2023 / 0.2404 (0.2367 / 0.2674)	0.1837 / 0.2384 (0.2299 / 0.2820)
Number of atoms				
Protein	12,784	12,848	12,618	6,664
Ligand/ion	30	43	71	28
Water	0	40	12	232
B factors	56.60	66.20	80.90	42.30
Protein	56.60	66.10	80.50	42.70
Ligand/ion	60.60	119.70	162.60	64.10
Water	–	41.40	39.70	30.60
r.m.s. deviations				
Bond lengths (Å)	0.008	0.007	0.010	0.009
Bond angles (°)	0.92	0.87	1.04	1.14

Values in parentheses are for highest-resolution shell.

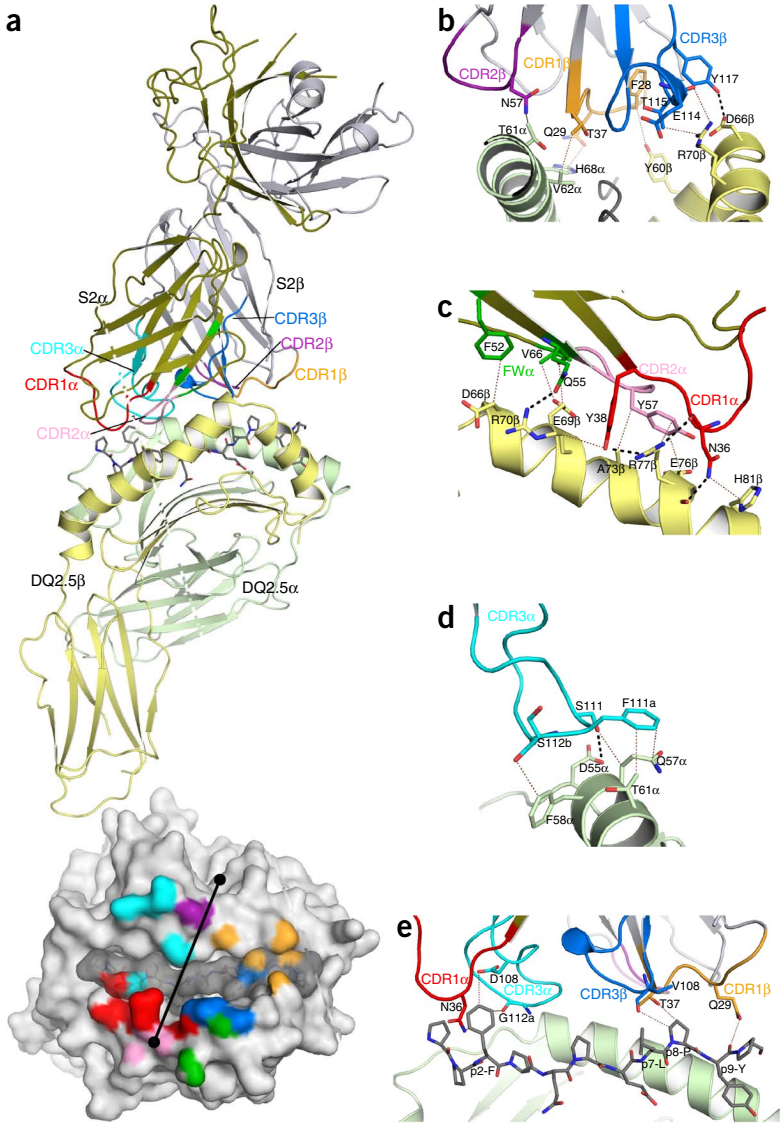

Figure 3 Interactions at the interface of S2 and HLA-DQ2-glia-α1a. (**a**) Overview of the S2–HLA-DQ2.5-glia-α1a complex with the peptide shown as gray sticks. Top, HLA-DQ2.5 α- and β-chains are light green and light yellow, respectively; the S2 α- and β-chains are dark yellow and light gray, respectively. CDRs are colored as follows: CDR1α, red; CDR2α, pink; CDR3α, cyan; CDR1β, orange; CDR2β, purple; and CDR3β, blue. Bottom, TCR footprint of the antigen binding interface. HLA-DQ2.5-glia-α1 is shown as a surface representation with the peptide in gray and TCR contact atoms colored according to nearest CDR loop. Framework contacts are colored green. The black dots and line represent the center of mass positions of the TCR variable domains and show the approximate TCR docking angle. (**b**) Interactions between the S2 β-chain and HLA-DQ2.5. Black dashes, hydrogen bonds; dotted lines, van der Waals interactions. All amino acids are indicated by their single-letter abbreviations. (**c**) Interactions between the S2 CDR1α loop and the HLA-DQ2.5 β-chain. (**d**) Largely apolar interactions between the S2 CDR3α loop and the HLA-DQ2.5 β-chain. (**e**) Interactions between the S2 TCR and the DQ2.5-glia-α1a peptide.

HLA-DQ2.5-glia-α1a recognition

To address the basis of HLA-DQ2.5-glia-α1a recognition, we determined the S2 TCR–HLA-DQ2.5-glia-α1a complex (**Table 2** and **Supplementary Fig. 1a**). The S2 TCR docked centrally over HLA-DQ2 at approximately 80° across the antigen-binding cleft, where the Vα and Vβ chains of the S2 TCR sat above the β- and α-helix of HLA-DQ2, respectively, thereby adopting the standard TCR-pMHC docking geometry (**Fig. 3a** and **Supplementary Table 1**)[34]. The S2 TCR–HLA-DQ2.5-glia-α1a interface had a buried surface area (BSA) of ~1,100 Å^2, with the Vα and Vβ domains contributing 60% and 40% to the BSA, respectively. All six CDR loops, as well as non-CDR residues (framework regions) from the Vα chain, contributed to the interaction (**Fig. 3a** and **Supplementary Table 1**), with the CDR1α, CDR2α and CDR3α loops contributing 17%, 9% and 22% to the BSA, respectively, whereas the CDR1β, CDR2β and CDR3β loops contributed 13%, 4% and 17%, respectively. Thus, in terms of BSA, the CDR3 loops contributed the most to the interaction with HLA-DQ2.5-glia-α1a.

The CDR1β loop interacted diffusely with HLA-DQ2, and the CDR2β interactions were limited (**Fig. 3b**). Thus, the germline-encoded regions of TRBV20-1*01 were non-ideally disposed to interact with HLA-DQ2. Nevertheless, the CDR3β loop was wedged between the α- and β-chains of HLA-DQ2, sat directly above the antigenic peptide (discussed below) and made a number of contacts with the β-chain of HLA-DQ2 (**Fig. 3b**).

The TRAV4*01-TRAJ4*01 chain of the S2 TCR interacted with both the α- and β-chains of HLA-DQ2, with the CDR1α and CDR2α loops contacting the β-chain, whereas the CDR3α loop interacted with the α-chain of HLA-DQ2. The TRAV4*01 chain was locked onto HLA-DQ2 by interdigitation of Tyr38α with Arg70 and Arg77 from the β-chain of HLA-DQ2 as well as by the formation of additional interactions with the HLA-DQ2 β-chain (**Fig. 3c** and **Supplementary Table 1**). These interactions were supplemented by polar-mediated interactions between Asn36α, Gln55α and Tyr57α from the TCR α-chain and Arg70β, Arg77β and additional residues from HLA-DQ2 (**Fig. 3c** and **Supplementary Table 1**). The CDR3α–HLA-DQ2–α-chain interaction site was less featured and was mostly apolar in character (**Fig. 3d** and **Supplementary Table 1**). Accordingly, the interactions mediated by the CDR1α and CDR2α loops suggested a basis for the TRAV4*01 bias observed in the HLA-DQ2.5-glia-α1a–restricted response. The interactions with the DQ2.5-glia-α1a determinant were unusual in that the central region of this peptide was devoid of contacts with the S2 TCR (**Fig. 3e**). This observation was largely attributable to a central void at the interface that was created by the CDR3α and CDR3β loops and a featureless central region of the DQ2.5-glia-α1a peptide. Indeed, the proline-rich nature of the DQ2.5-glia-α1a epitope lends itself toward a mostly featureless determinant (**Fig. 3e**). Here the P7 leucine lay flat and was oriented toward the HLA-DQ2 β-chain helix, and thus the observation that substitution of the P7 leucine with alanine abrogates TCR recognition is most likely attributable to indirect structural effects. P2 phenylalanine, which protruded outwards, represented the most prominent region of the DQ2.5-glia-α1a epitope. Here, P2 phenylalanine contacted the CDR1α and CDR3α loops, whereas the main chain of the CDR3β loop sat above and contacted the

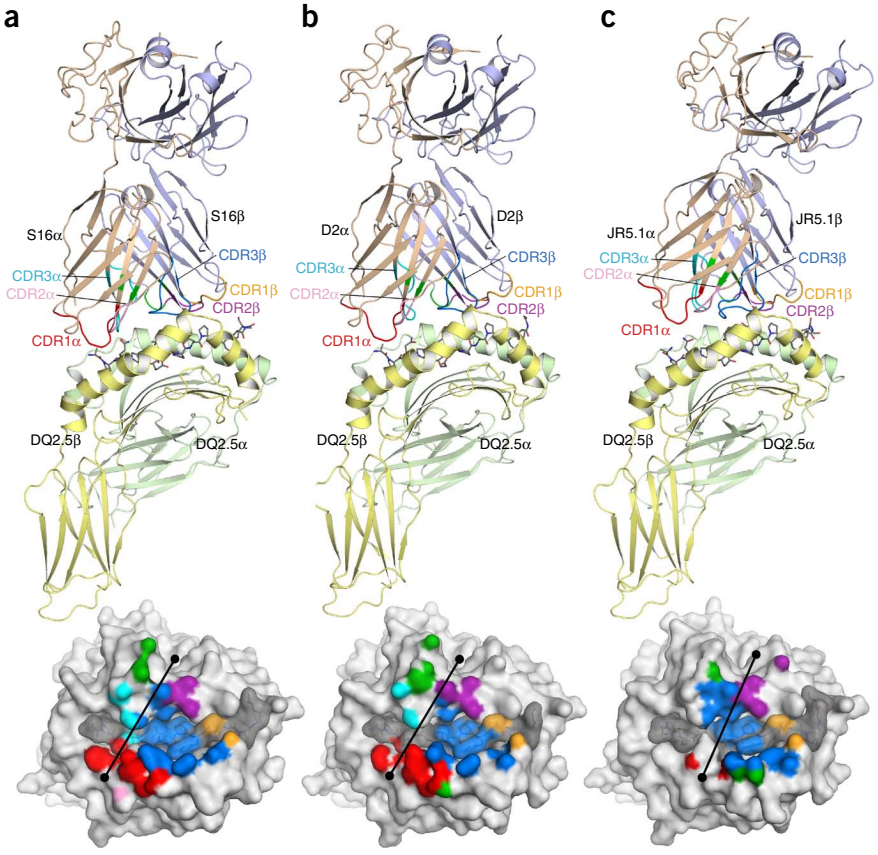

Figure 4 Docking of TRBV7-2 TCRs onto HLA-DQ2.5-glia-α2. (**a**–**c**) Structural overviews of TRAV26-1–TRBV7-2 TCR–HLA-DQ2.5-glia-α2 complexes with the TCRs S16 (**a**), D2 (**b**) and JR5.1 (**c**). HLA-DQ2.5 α- and β-chains are colored light green and light yellow, respectively, the TCR TRAV26-1 is colored in beige, and TRBV7-2 is in blue-gray. CDR1α, CDR2α and CDR3α are colored red, pink and cyan, respectively, and CDR1β, CDR2β and CDR3β are colored orange, purple and blue, respectively. The surfaces shown below are TCR footprints of the antigen-binding interfaces. HLA-DQ2.5-glia-α2 is shown as a surface representation with the peptide in gray and TCR contact atoms colored according to nearest CDR loop. The interconnected dots represent the center of mass positions of the TCR variable domains and show the approximate TCR docking angle.

C-terminal region of the epitope (**Fig. 3e**). In agreement, substitution of phenylalanine with alanine affected T-cell recognition (**Fig. 1a**). Accordingly, DQ2.5-glia-α1a is a mostly featureless gliadin determinant that results in suboptimal interactions with the S2 TCR.

HLA-DQ2.5-glia-α2 recognition

We next determined the basis of biased TRAV26-1*01–TRBV-7-2*01 (S16, D2 and JR5.1) TCR recognition against HLA-DQ2 presenting the DQ2.5-glia-α2 determinant (**Fig. 4a–c**, **Table 2** and **Supplementary Fig. 1b–d**). These three TCRs possess differing CDR3 loops, thereby providing insight into biased TRAV and TRBV usage in a range of contexts. We first describe the S16 TCR ternary complex and compare it to the distinguishing features of the D2 TCR and JR5.1 TCR–HLA-DQ2.5-glia-α2 ternary complexes. The S16 TCR docked 70° relative to the HLA-DQ2 antigen-binding cleft, burying approximately 1,060 Å^2 on complexation, in which the α- and β-chains of the TCR were positioned over the β- and α-helices of HLA-DQ2, respectively (**Fig. 4a** and **Supplementary Table 2**). The TCR β-chain contributed 60% of the BSA at the interface, thereby suggesting why the TRBV7-2 chain predominates in the DQ2.5-glia-α2–restricted response. Surprisingly, however, after binding, the CDR1β and CDR2β loops and the TRBV7-2 framework region contributed only 6%, 8% and 10% of the BSA, respectively. Indeed, the CDR1β loop does not appreciably contact HLA-DQ2 (**Supplementary Table 2**), and interactions through the CDR2β loop and framework contacts were limited (**Fig. 5a**).

The CDR1α, CDR2α and CDR3α loops contributed 20%, 7% and 11% of the BSA, respectively, at the S16 TCR–HLA-DQ2.5-glia-α2 interface. Tyr38α from the CDR1α loop slotted in between Arg70β and Arg77β of HLA-DQ2 (**Fig. 5b**) in a manner analogous to how Tyr38α from the HLA-DQ2.5-glia-α1a–specific TRAV4*01$^+$ S2 TCR interacted with HLA-DQ2 (**Fig. 3c**). Moreover, a neighboring Tyr40α interacted with Arg70β, and Asn36α contacted Arg77β and His81β, with this latter interaction resonating with the corresponding TRAV4*01$^+$ S2 TCR–HLA-DQ2.5-glia-α1a interaction (**Figs. 5b** and **3c**). The CDR2α loop was peripherally located at the HLA-DQ2.5-glia-α2 interface (**Fig. 4a**). The CDR3α loop, although more centrally disposed, did not make extensive contacts with HLA-DQ2 (data not shown).

The non–germline encoded CDR3β loop sat centrally atop HLA-DQ2.5-glia-α2 and was the principal contact zone for the S16 TCR, with polar contacts predominating (**Fig. 5c**). Namely, the CDR3β loop contributed 35% of the BSA on binding and interacted with the peptide (discussed below) and both chains of the HLA-DQ2 molecule (**Fig. 4a**). The CDR3β loop sat above the DQ2.5-glia-α2 peptide, with the tip of the loop pointing toward the helix of HLA-DQ2's α-chain (**Fig. 5c**). The main contributor to the CDR3β-HLA-DQ2–mediated interactions was Arg109β, which arched down into the antigen-binding cleft and interacted with the peptide, whereas its aliphatic moiety packed against Val65α, and its guanidinium group hydrogen bonded to Thr61α and Asn62α of HLA-DQ2 (**Fig. 5c**).

In agreement with the results of the functional analyses (**Fig. 1c**), the S16 TCR contacted all three of the prominent upward-pointing residues (P2 glutamine, P5 leucine and P7 tyrosine) of the DQ2.5-glia-α2 peptide, as well as forming interactions with the main chain of P6 proline and P8 proline (**Fig. 5d**). The P7 tyrosine hydrogen bonded to Asp114β from the CDR3β loop and packed against the aliphatic moiety of Arg109β. The Arg109β residue lay against the main chain of P6 and packed against P5 leucine. However, Arg109β did not contact the deamidated P4 glutamic acid residue. Thus, the non–germline encoded arginine residue has a central role in interacting with HLA-DQ2.5-glia-α2.

Impact of CDR3 hypervariability

The D2 TCR and S16 TCRs docked very similarly onto HLA-DQ2.5-α-glia2, with an overall r.m.s. deviation between the complexes of 0.8 Å^2 and with the center of mass of the Vα and Vβ domains differing by only 0.4 and 0.8 Å, respectively (**Fig. 4b**). As such, the interatomic contacts mediated by the CDR1 and CDR2 loops

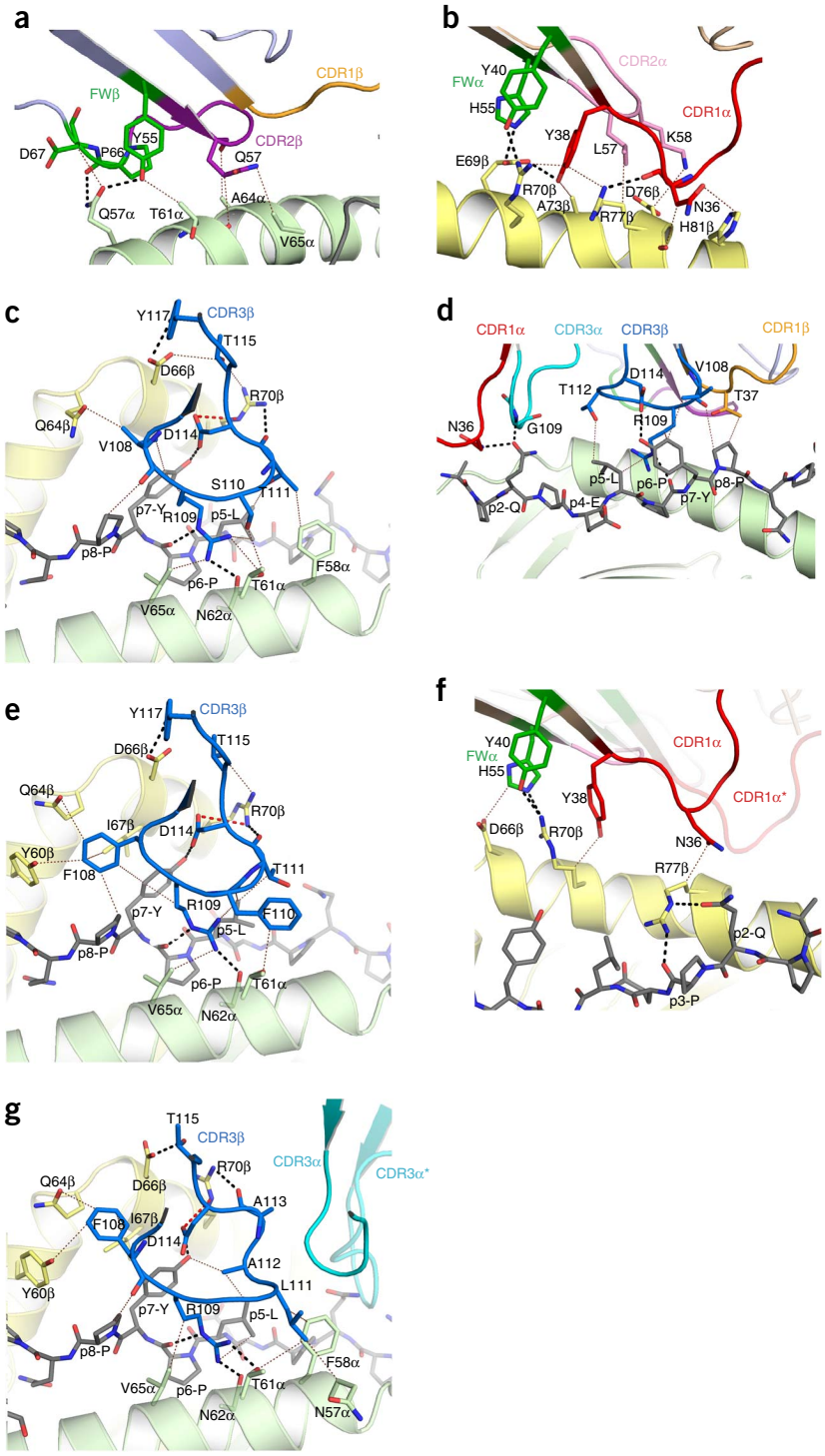

Figure 5 Interactions at the TCR–HLA-DQ2.5-glia-α2 interface. (**a**) The S16 CDR2β loop (purple) and adjacent Vβ framework residues (green) with HLA-DQ2.5-glia-α2 (light green). (**b**) The S16 CDR1α loop (red) and HLA-DQ2.5-glia-α2 (light yellow) supplemented by CDR2α (pink) and adjacent framework residues (green). (**c**) The S16 CDR3β loop (blue) and HLA-DQ2.5-glia-α2 (light yellow and light green). (**d**) S16 (red, cyan, blue, purple and orange) and the glia-α2 peptide (gray). (**e**) The D2 CDR3β loop (blue) and HLA-DQ2.5-glia-α2 (light yellow and light green). (**f**) The JR5.1 CDR1α loop (red) and HLA-DQ2.5-glia-α2 (light yellow) supplemented by Vα framework residues (green). The position of the S16 TCR (CDR1α*, semi-transparent) is overlaid for comparison, showing the relative uplift of the JR5.1 α-chain. (**g**) The JR5.1 CDR3β loop (blue) and HLA-DQ2.5-glia-α2 (light yellow and light green). The added length of the JR5.1 CDR3β loop influences docking of the TCR α-chain and limits the space available for CDR3α (cyan). The CDR3α of the superimposed S16 TCR (CDR3α*, semi-transparent) is shown for comparison. HLA-DQ2.5 α- and β-chains are colored light green and light yellow, respectively. Black dashes, hydrogen bonds; red dashes, salt bridges; dotted lines, van der Waals interactions. All amino acids are indicated by their single-letter abbreviations.

are largely conserved, including the Tyr38α from the CDR1α loop that wedged between Arg70β and Arg77β (**Supplementary Tables 2** and **3**). Moreover the shorter CDR3α loop of the D2 TCR does not appreciably affect its footprint on HLA-DQ2.5-glia-α2 (**Fig. 4b**). The CDR3β-mediated contacts of the D2 TCR were more extensive (41% BSA) than those of the S16 TCR, a difference that was attributable to the presence of two bulky aromatics (Phe108β and Phe110β in the D2 TCR compared to Val108β and Ser110β in the S16 TCR) (**Fig. 5e**). Notably, Arg109β and Asp114β from the CDR3β loop of the D2 TCR were involved in essentially the same interactions as those observed in the S16 TCR ternary complex, and thus the core interactions with the DQ2.5-glia-α2 determinant are conserved between these two TCRs (**Fig. 5c**,**e**).

Whereas the CDR3α loop of the JR5.1 TCR was the same length as that of the D2 TCR, the CDR3β loop of the JR5.1 TCR was two residues longer than those of the S16 and D2 TCRs (**Table 1**). This variation in CDR3β loop length had a surprising impact on HLA-DQ2.5-glia-α2 recognition. The corresponding Vβ chains of the JR5.1, S16 and D2 TCRs are located equivalently (r.m.s. deviations of 3.5 and 3.4 Å, respectively), and although the interactions with Tyr55β are lost in the JR5.1 TCR ternary complex, the interactions mediated by Thr37β, Gln57β and Pro66β are nevertheless largely conserved (**Supplementary Table 4**).

However, the corresponding Vα chains of the JR5.1, S16 and D2 TCRs were not located equivalently (r.m.s. deviations of 7.1 and 6.8 Å, respectively). Here, the JR5.1 TCR was lifted away from HLA-DQ2.5-glia-α2, and thus the extent of contacts mediated by the α-chain of the JR5.1 TCR was markedly diminished (BSA of 230 $Å^2$ compared to BSA of 420 $Å^2$) (**Fig. 4c**). In comparison to the S16 TCR complex, the equivalent Vα domains of the S16 and JR5.1 TCRs differ in their center of gravity by 4.8 Å (**Fig. 4c**). As a consequence, the interactions with the CDR2α and CDR3α loops were essentially lost in the JR5.1 TCR ternary complex, whereas Tyr38α from the CDR1α loop, although being displaced by approximately 3 Å, retained a finger-grip hold on HLA-DQ2, with its aromatic ring stacked against the aliphatic moiety of Arg70β (**Fig. 5f**). The reason for this marked rejuxtaposition

Table 3 Binding affinities of D2 TCR mutants for HLA-DQ2.5-glia-α2

	K_d (μM)[a]
D2	15.8 ± 0.4
α–Asn36Ala	14.0 ± 0.5
α–Tyr38Ala	>300
α–Tyr40Phe	>300
α–Leu57Ala	116.8 ± 14.5
β–Tyr55Phe	5.3 ± 0.4
β–Gln57Ala	61.5 ± 5.5
β–Asn63Ala	13.1 ± 0.6
β–Phe108Ala	178.2 ± 21.2
β–Arg109Ala	>300
β–Phe110Ala	70.2 ± 4.2
β–Asp114Ala	256.2 ± 59.9
β–Tyr117Phe	38.9 ± 1.5

[a]K_d values obtained by SPR as described in the Online Methods, with s.d. from *n* replicate measurements derived from two independent experiments, as shown in **Supplementary Figure 2**.

of the JR5.1 Vα chain is the presence of the longer CDR3β loop, which abutted the CDR3α loop, thereby forcing the Vα chain away to avoid steric clashes with the CDR3β loop. Nevertheless, despite this CDR3β loop variation, Asp114β maintained the hydrogen bond with P7 tyrosine of DQ2.5-glia-α2 and a salt bridge with Arg70β (**Fig. 5g**). Moreover, Arg109β was located in essentially the identical position and formed a very similar network of interactions in the three HLA-DQ2.5-glia-α2–restricted TCRs (**Fig. 5g**). Thus, Arg109β from the CDR3β loop acted as the lynchpin that mediated recognition with HLA-DQ2.5-glia-α2.

Energetics underpinning DQ2.5-glia-α2 recognition

Next, to provide insight into the basis for the *TRBV7-2* and *TRAV26-2* bias and the importance of CDR3-mediated contacts in DQ2.5-glia-α2 recognition, we undertook an alanine-scanning mutagenesis and SPR approach[35] using the D2 TCR–HLA-DQ2.5-glia-α2 structure as a guide. In total, we chose 13 single-site mutants of D2 TCR for analysis, with the choice being dictated by the residue forming contacts with DQ2.5-glia-α2 and the residue being unlikely to affect the stability of the D2 TCR (**Table 3** and **Supplementary Fig. 2**). All of the TCR mutants except one (H55αA) were expressed and refolded well and adopted a fully folded conformation as judged by comparing their chromatographic properties to those of the wild-type refolded D2 TCR (data not shown). We determined the effect of mutations on TCR recognition of HLA-DQ2.5-glia-α2 using SPR analysis. We assigned the effects of the D2 TCR mutants into three categories: no effect, moderate effect (K_d between 47.3 and 78.9 μM) and marked effect (K_d > 78.9 μM or K_d < 3.2 μM) (**Table 3** and **Supplementary Fig. 2**).

Although N36αA had no effect on D2 TCR recognition, mutation of the germline-encoded residues Tyr38α, Tyr40α and Leu57α markedly affected D2 TCR recognition of HLA-DQ2.5-glia-α2, indicating their pivotal role in the TRAV26-1 bias (**Table 3** and **Supplementary Fig. 2**).

Of the mutations in the germline-encoded residues of the D2 TCR β-chain, Q57βA moderately affected HLA-DQ2.5-glia-α2 recognition, and, surprisingly, Y55βF caused an approximate three-fold increase in the affinity for HLA-DQ2.5-glia-α2 (**Table 3** and **Supplementary Fig. 2**). In contrast, the majority of the mutations in the CDR3β loop affected D2 TCR recognition. Namely, whereas the F110βA mutation moderately affected HLA-DQ2.5-glia-α2 recognition, the R109βA, F108βA and D114βA mutations had marked effects on binding of the D2 TCR with HLA-DQ2.5-glia-α2. Accordingly, the germline-encoded regions of the TCR α-chain and non–germline encoded regions of the TCR β-chain have a crucial energetic role in mediating contacts with HLA-DQ2.5-glia-α2.

DISCUSSION

Here we provide detailed insight into how the responding T-cell repertoire interacts with two immunodominant gliadin determinants that are presented by HLA-DQ2, thereby providing an understanding of the fundamental molecular basis underpinning CD.

The response to the DQ2.5-glia-α1a determinant was characterized by biased *TRAV4*01* and *TRBV20-1* or *TRBV29-1* usage, whereas that against the DQ2.5-glia-α2 determinant was biased toward *TRAV26-1–TRBV7-2* TCR usage[26–28]. Interestingly, in the HLA-DQ8–mediated form of the disease, biased *TRBV9-1* usage has been observed[25], thereby indicating that the gliadin-restricted HLA-DQ2 and HLA-DQ8 determinants appear to preferentially select αβ T cells from the available repertoire, and the corresponding TCRs could potentially represent defining characteristics for these diseases. In this respect, it is important to note that disease symptoms associated with CD are highly variable, and disease can in essence develop at any age[3]. Moreover, Bodd *et al.*[36] reported that the frequency of gluten-specific T cells correlated with Marsh score, a measure of damage in the gut mucosa. Thus, it is tempting to speculate that the appearance and frequency of T cells expressing a biased T-cell repertoire specific for immunodominant gliadin peptides may determine disease onset and/or severity.

Notably, the affinity of the HLA-DQ8–restricted TCRs[25] seemed to be, on average, higher than that of the HLA-DQ2–restricted TCRs. In line with the view that autoreactive TCRs can stabilize low-affinity peptide–MHC complexes[37], it is conceivable that these observations are linked to the more stringent deamidation dependence of the HLA-DQ2–restricted epitopes in comparison to the HLA-DQ8–restricted gliadin determinants. The TRBV7-2–mediated interactions with HLA-DQ2 were not extensive, suggesting that biased TCR β-chain usage may also partially relate to preferential TCR α-chain pairing[38,39]. Nevertheless, the corresponding TRBV7-2 footprint on HLA-DQ2 was maintained in three distinct TRBV7-2$^+$ ternary complexes, suggesting an important role of the TCR β-chain in mediating docking.

The TRAV4*01$^+$ TCR docking onto HLA-DQ2.5-glia-α1a differed from that of the HLA-DQ2.5-glia-α2–restricted TCRs examined, with the differences in docking geometries presumably reflecting the varied TCR gene usage as well as the markedly different nature of the DQ2.5-glia-α1a and DQ2.5-glia-α2 sequences. The *TRAV4*01* bias against HLA-DQ2.5-glia-α1a appeared to be attributable mostly to an Asn36–Tyr38 motif within the CDR1α loop and Tyr57α from the CDR2α loop. Interestingly, although the corresponding sequence of the CDR1α loop of the TRAV26-1 chain differed from that of the TRAV4*01$^+$ TCR, it also possessed an Asn36–Tyr38 motif, which formed an analogous set of interactions with HLA-DQ2 when presenting the DQ2.5-glia-α2 determinant. Collectively, these observations suggest a common mode relating to *TRAV4*01* and *TRAV26-1* bias toward HLA-DQ2. However, the molecular determinants underpinning this TRAV-mediated bias can be disrupted by subtle modifications within the non–germline encoded regions of the HLA-DQ2–restricted TCRs. This result simultaneously highlights the precarious nature and the limited role of germline-encoded interactions with HLA-DQ2.

In contrast, the CDR3 loops of the DQ2-restricted TCRs had a major role in mediating their interactions with HLA-DQ2-glia-α1a and HLA-DQ2.5-glia-α2. In the HLA-DQ2.5-glia-α1a–restricted response, the CDR3α and CDR3β loops made numerous interactions with the HLA-DQ2 molecule itself, as well as contacting the featureless DQ2.5-glia-α1a determinant. Regarding the

HLA-DQ2.5-glia-α2–restricted response, the CDR3β loop had a pivotal role in interacting with DQ2.5-glia-α2 as well as HLA-DQ2. In particular, the conservation of the location of Arg109β and its corresponding interaction network across three distinct TCRs was striking. The observation of a highly conserved arginine in the HLA-DQ2.5-glia-α2–restricted response had resonances with the strong conservation, and essential energetic role, of a non–germline encoded arginine residue within the CDR3α loop of TCRs restricted toward HLA-DQ8-glia-α1 (ref. 25). Thus, although TCR bias is observed in HLA-DQ2– and HLA-DQ8–mediated CD, it is the frequent presence of a non–germline encoded arginine residue that has the key role in mediating recognition of gliadin determinants presented by HLA-DQ2 or HLA-DQ8. Collectively, these observations point to stringent selection of a high-affinity TCR repertoire and as such not only offer key insight into the pathogenesis of CD and antigen-specific immunotherapy to treat CD[40] but also may be of relevance for our understanding of the involvement of biased T-cell repertoire selection in other HLA-associated disorders.

METHODS

Methods and any associated references are available in the online version of the paper.

Accession codes. Coordinates and structure factors have been deposited in the Protein Data Bank under the following accession codes: S2 TCR–DQ2.5-glia-α1a, 4OZI; S16 TCR–HLA-DQ2α2, 4OZH; D2 TCR–HLA-DQ2α2, 4OZG; JR5.1 TCR–HLA-DQ2α2, 4OZF.

Note: Any Supplementary Information and Source Data files are available in the online version of the paper.

ACKNOWLEDGMENTS

We thank the staff of the Monash crystallization facility and the Australian Synchrotron for assistance with crystallization and data collection, respectively. This work was supported by the Australian Research Council, the National Health and Medical Research Council (NHMRC) of Australia, the Celiac Disease Consortium and an Innovative Cluster approved by The Netherlands Genomics Initiative and was funded in part by the Dutch government (grant BSIK03009). We thank J. Tye-Din for assistance. J.R. is supported by an Australia Fellowship from the NHMRC.

AUTHOR CONTRIBUTIONS

J.P. and V.M. are joint first authors. J.R.M., K.L.L., D.X.B., M.v.L., A.T., M.L.M., J.S., Y.K.-W., J.v.B., J.W.D., W.-T.K., N.L.L.G. and R.P.A. performed experiments, provided key reagents and/or analyzed data and/or provided intellectual input or helped write the manuscript. H.H.R., F.K. and J.R. are joint senior and corresponding authors, co-led the investigation and contributed to the design and interpretation of data, project management and writing of the manuscript.

COMPETING FINANCIAL INTERESTS

The authors declare competing financial interests: details are available in the online version of the paper.

1. Abadie, V., Sollid, L.M., Barreiro, L.B. & Jabri, B. Integration of genetic and immunological insights into a model of celiac disease pathogenesis. *Annu. Rev. Immunol.* **29**, 493–525 (2011).
2. Jabri, B. & Sollid, L.M. Tissue-mediated control of immunopathology in coeliac disease. *Nat. Rev. Immunol.* **9**, 858–870 (2009).
3. Di Sabatino, A. & Corazza, G.R. Coeliac disease. *Lancet* **373**, 1480–1493 (2009).
4. Sollid, L.M. Coeliac disease: dissecting a complex inflammatory disorder. *Nat. Rev. Immunol.* **2**, 647–655 (2002).
5. Sollid, L.M. & Jabri, B. Triggers and drivers of autoimmunity: lessons from coeliac disease. *Nat. Rev. Immunol.* **13**, 294–302 (2013).
6. Petersen, J., Purcell, A. & Rossjohn, J. Post-translationally modified T cell epitopes: immune recognition and immunotherapy. *J. Mol. Med.* **87**, 1045–1051 (2009).
7. Karell, K. *et al.* HLA types in celiac disease patients not carrying the DQA1*05–DQB1*02 (DQ2) heterodimer: results from the European Genetics Cluster on Celiac Disease. *Hum. Immunol.* **64**, 469–477 (2003).
8. Shan, L. *et al.* Structural basis for gluten intolerance in celiac sprue. *Science* **297**, 2275–2279 (2002).
9. Henderson, K.N. *et al.* A structural and immunological basis for the role of human leukocyte antigen DQ8 in celiac disease. *Immunity* **27**, 23–34 (2007).
10. Kim, C.Y., Quarsten, H., Bergseng, E., Khosla, C. & Sollid, L.M. Structural basis for HLA-DQ2–mediated presentation of gluten epitopes in celiac disease. *Proc. Natl. Acad. Sci. USA* **101**, 4175–4179 (2004).
11. Molberg, O. *et al.* Tissue transglutaminase selectively modifies gliadin peptides that are recognized by gut-derived T cells in celiac disease. *Nat. Med.* **4**, 713–717 (1998).
12. van de Wal, Y. *et al.* Selective deamidation by tissue transglutaminase strongly enhances gliadin-specific T cell reactivity. *J. Immunol.* **161**, 1585–1588 (1998).
13. Tollefsen, S. *et al.* HLA-DQ2 and -DQ8 signatures of gluten T cell epitopes in celiac disease. *J. Clin. Invest.* **116**, 2226–2236 (2006).
14. van de Wal, Y. *et al.* Glutenin is involved in the gluten-driven mucosal T cell response. *Eur. J. Immunol.* **29**, 3133–3139 (1999).
15. van de Wal, Y. *et al.* Small intestinal T cells of celiac disease patients recognize a natural pepsin fragment of gliadin. *Proc. Natl. Acad. Sci. USA* **95**, 10050–10054 (1998).
16. Arentz-Hansen, H. *et al.* The intestinal T cell response to α-gliadin in adult celiac disease is focused on a single deamidated glutamine targeted by tissue transglutaminase. *J. Exp. Med.* **191**, 603–612 (2000).
17. Arentz-Hansen, H. *et al.* Celiac lesion T cells recognize epitopes that cluster in regions of gliadins rich in proline residues. *Gastroenterology* **123**, 803–809 (2002).
18. Qiao, S.W. *et al.* Tissue transglutaminase-mediated formation and cleavage of histamine-gliadin complexes: biological effects and implications for celiac disease. *J. Immunol.* **174**, 1657–1663 (2005).
19. Vader, W. *et al.* The gluten response in children with celiac disease is directed toward multiple gliadin and glutenin peptides. *Gastroenterology* **122**, 1729–1737 (2002).
20. Anderson, R.P., Degano, P., Godkin, A.J., Jewell, D.P. & Hill, A.V.S. *In vivo* antigen challenge in celiac disease identifies a single transglutaminase-modified peptide as the dominant A-gliadin T-cell epitope. *Nat. Med.* **6**, 337–342 (2000).
21. Henderson, K.N. *et al.* The production and crystallization of the human leukocyte antigen class II molecules HLA-DQ2 and HLA-DQ8 complexed with deamidated gliadin peptides implicated in coeliac disease. *Acta Crystallogr. Sect. F Struct. Biol. Cryst. Commun.* **63**, 1021–1025 (2007).
22. Vader, L.W. *et al.* Characterization of cereal toxicity for celiac disease patients based on protein homology in grains. *Gastroenterology* **125**, 1105–1113 (2003).
23. Vader, W. *et al.* The HLA-DQ2 gene dose effect in celiac disease is directly related to the magnitude and breadth of gluten-specific T cell responses. *Proc. Natl. Acad. Sci. USA* **100**, 12390–12395 (2003).
24. Tye-Din, J.A. *et al.* Comprehensive, quantitative mapping of T cell epitopes in gluten in celiac disease. *Sci. Transl. Med.* **2**, 41ra51 (2010).
25. Broughton, S.E. *et al.* Biased T cell receptor usage directed against human leukocyte antigen DQ8-restricted gliadin peptides is associated with celiac disease. *Immunity* **37**, 611–621 (2012).
26. Qiao, S.W., Christophersen, A., Lundin, K.E. & Sollid, L.M. Biased usage and preferred pairing of α- and β-chains of TCRs specific for an immunodominant gluten epitope in coeliac disease. *Int. Immunol.* **26**, 13–9 (2014).
27. Qiao, S.W. *et al.* Posttranslational modification of gluten shapes TCR usage in celiac disease. *J. Immunol.* **187**, 3064–3071 (2011).
28. Han, A. *et al.* Dietary gluten triggers concomitant activation of CD4+ and CD8+ αβ T cells and γδ T cells in celiac disease. *Proc. Natl. Acad. Sci. USA* **110**, 13073–13078 (2013).
29. Turner, S.J., Doherty, P.C., McCluskey, J. & Rossjohn, J. Structural determinants of T-cell receptor bias in immunity. *Nat. Rev. Immunol.* **6**, 883–894 (2006).
30. Gras, S., Kjer-Nielsen, L., Burrows, S.R., McCluskey, J. & Rossjohn, J. T-cell receptor bias and immunity. *Curr. Opin. Immunol.* **20**, 119–125 (2008).
31. Godfrey, D.I., Rossjohn, J. & McCluskey, J. The fidelity, occasional promiscuity, and versatility of T cell receptor recognition. *Immunity* **28**, 304–314 (2008).
32. Yin, Y., Li, Y. & Mariuzza, R.A. Structural basis for self-recognition by autoimmune T-cell receptors. *Immunol. Rev.* **250**, 32–48 (2012).
33. Bulek, A.M. *et al.* Structural basis for the killing of human β cells by CD8+ T cells in type 1 diabetes. *Nat. Immunol.* **13**, 283–289 (2012).
34. Gras, S. *et al.* A structural voyage toward an understanding of the MHC-I–restricted immune response: lessons learned and much to be learned. *Immunol. Rev.* **250**, 61–81 (2012).
35. Borg, N.A. *et al.* The CDR3 regions of an immunodominant T cell receptor dictate the 'energetic landscape' of peptide-MHC recognition. *Nat. Immunol.* **6**, 171–180 (2005).
36. Bodd, M. *et al.* Direct cloning and tetramer staining to measure the frequency of intestinal gluten-reactive T cells in celiac disease. *Eur. J. Immunol.* **43**, 2605–2612 (2013).
37. Yin, Y., Li, Y., Kerzic, M.C., Martin, R. & Mariuzza, R.A. Structure of a TCR with high affinity for self-antigen reveals basis for escape from negative selection. *EMBO J.* **30**, 1137–1148 (2011).
38. Stadinski, B.D. *et al.* A role for differential variable gene pairing in creating T cell receptors specific for unique major histocompatibility ligands. *Immunity* **35**, 694–704 (2011).
39. Turner, S.J. & Rossjohn, J. αβ T cell receptors come out swinging. *Immunity* **35**, 660–662 (2011).
40. Anderson, R.P. & Jabri, B. Vaccine against autoimmune disease: antigen-specific immunotherapy. *Curr. Opin. Immunol.* **25**, 410–417 (2013).
41. Sollid, L.M., Qiao, S.W., Anderson, R.P., Gianfrani, C. & Koning, F. Nomenclature and listing of celiac disease relevant gluten T-cell epitopes restricted by HLA-DQ molecules. *Immunogenetics* **64**, 455–460 (2012).

ONLINE METHODS

Antigens and peptides. A pepsin and trypsin digest of gluten (Sigma Chemical, St. Louis, USA) was prepared as described[15]. Peptides were synthesized by standard Fmoc chemistry on a multiple peptide synthesizer (Syroll, MultiSynTech GmbH, Witten, Germany). The integrity of the peptides was verified by reverse-phase HPLC and mass spectrometry. Tissue transglutaminase (TG2) treatment was performed by incubating the pepsin- and trypsin-treated gluten digest with TG2 (Sigma) in 50 mM triethylalamine-acetate (pH 6.5) and 2 mM $CaCl_2$ at 37 °C for 4 h as described[12].

Gluten-specific T-cell lines and clones. Polyclonal gluten-specific T-cell lines were isolated from the small intestine of patients with CD as described[19]. In short, biopsies were cultured with a mixture of gluten and TG2-treated gluten for 5 d. Subsequently, IL-2 (20 Cetus units/ml; Novartis, Arnhem, The Netherlands) and IL-15 (10 ng/ml; R&D systems, Abingdon, UK) were added to expand the T cells. Re-stimulation was performed with mixed irradiated allogeneic PBMCs in the presence of phytohemagglutinin (1 µg/ml; Remel Inc. Lenexa, USA), IL-2 (20 Cetus units/ml) and IL-15 (10 ng/ml). The resulting T-cell lines were stored in liquid nitrogen and later tested for reactivity against a pepsin and trypsin digest of gluten and a pepsin and trypsin digest of gluten treated with TG2 in a T-cell proliferation assay. Gluten-reactive lines were cloned by limiting dilution and were again expanded by re-stimulation at 1- to 3-week intervals. Clones were stored in liquid nitrogen. The HLA-DQ2.5-glia-α2–restricted JR5.1 clone was derived from the small intestine of a patient with CD (clone 3 in ref. 24). The HLA-DQ2.5-glia-α1a–restricted LS2.8/3.15 clone was derived from the peripheral blood of a gluten-challenged patient (clone 2 in ref. 24).

T-cell proliferation assays. Proliferation assays were performed in triplicate in 150 µl Iscove's modified Dulbecco's medium supplemented with glutamine (Gibco) and 10% human serum in 96-well flat-bottom plates. Briefly, antigen-presenting cells (APCs) were loaded with antigen for 2 h, after which 20,000 T cells were added. As APCs we used 10^5 irradiated HLA-DQ2–matched allogeneic PBMCs (3,000 rad). Unless otherwise indicated, TG2-treated gliadin was used at a final concentration of 450 µg/ml, and synthetic peptides were used at a final concentration of 6 µg/ml. After 48 h at 37 °C, cultures were pulsed with 0.5 µCi of ^{3}H-thymidine and harvested 18 h later. The peptides used were 13-mer versions of the DQ2.5-glia-α1a (LQ**PFPQPELPY**PQ, with the nine-amino-acid core in bold) and DQ2.5-glia-α2 (PF**PQPEPLYPQ**PQ, with the nine-amino-acid core in bold) epitopes and single alanine substitution versions thereof.

Isolation and sequencing of TCRs. With the exception of JR5.1, total RNA was isolated from T-cell clones by employing the RNeasy Mini Kit (Qiagen) and cDNA synthesized using superscript reverse transcriptase III (Invitrogen, USA) following the manufacturer's instructions. TCR β and α gene usage was determined with a set of specifically designed PCR primers. PCR products encoding all TCRs were cloned into the pGEM-T Easy vector (Promega) and sequenced. The αβ TCR gene usage and CDR3 sequences for all clones were determined using IMGT/V-QUEST[42]. The cDNA sequences encoding the α- and β-chain of the JR5.1 and LS2.8/3.15 TCRs were determined using a nested multiplex PCR strategy, as described[43], on individual cells producing IFN-γ in response to peptide stimulation with HLA-DQ2$^+$ B lymphoblastoid cell lines as APCs.

Mutagenesis, protein expression and purification. TCRs with a disulfide linkage engineered in their constant domains were expressed in *Escherichia coli* BL21(DE3), refolded and purified as described previously[44]. Mutants of the D2 TCR were produced by replacing the coding region for the TCR variable domains with synthetic gene fragments carrying the respective mutation. High Five insect cells (Trichoplusia ni BTI-TN-5B1-4 cells, Invitrogen) were used to coexpress soluble extracellular domains of the HLA-DQ2.5 α- and β-chains in a baculovirus expression system essentially as previously described[9,25]. Briefly, baculovirus HLA-DQ2.5 expression constructs had enterokinase-cleavable Fos and Jun zippers at the C-terminal ends of the α- and β-chain, respectively, to promote dimerization. The C terminus of the β-chain also included a BirA recognition sequence for biotinylation, as described previously[25], as well as a histidine tag for purification using immobilized metal ion affinity chromatography. Before crystallization, the Fos and Jun zippers were removed by enterokinase (Genscript) digestion, followed by separation using anion exchange chromatography (HiTrap Q HP, GE Healthcare). Purified TCRs were mixed at a 1:1 ratio with purified HLA-DQ2.5-glia-α2 (D2, JR5.1 and S16) or HLA-DQ2.5-glia-α1a (S2) and concentrated for crystallization.

Crystallization, data collection and processing. Crystallization was carried out using the hanging-drop vapor-diffusion method at 20 °C. All four TCR–HLA-DQ2.5-gliadin complexes were concentrated to 6–9 mg/ml in 10 mM Tris, pH 8, and 150 mM NaCl. Diffraction quality crystals of all complexes were obtained in similar conditions using 0.15–0.25 M CaOAc, 0.1 M Tris, pH 8.0–8.5, and 12–18% PEG 3350 as mother liquor, and crystallization droplets were set up by adding 0.2–0.3 µl of a solution containing 10 mM oxidized and 10 mM reduced glutathione to 0.5 µl of the mother liquor, followed by addition of 0.5 µl of protein solution. Crystals typically appeared within 2–3 d and grew to maximal size within 2 weeks. Before flash freezing in liquid nitrogen, crystals were cryoprotected by gradual transfer into mother liquor supplemented with 17% ethylene glycol. Data sets were collected at 100 K on the MX2 beamline of the Australian Synchrotron (Clayton, Victoria)[45] using an ADSC Quantum 315r detector. Data processing was carried out with Mosflm and Scala from the CCP4 program suite[46]. In the case of the S16 HLA-DQ2.5-glia-α2 complex, data were processed using the automated implementation of XDS[47] at the Australian Synchrotron.

Structure determination, refinement and validation. Initially, the ternary complex structure of JR5.1-HLA-DQ2.5-glia-α2 was solved by molecular replacement in PHASER[48] using the coordinates of the SP3.4 TCR[25] and of HLA-DQ2-glia-α1a[10] as search models with the peptide and CDR loops removed. The other three ternary complexes were solved using the components of the refined JR5.1-HLA-DQ2.5-glia-α2 structure. The refinement procedure followed the same protocol in all cases. Initially, iterative rounds of model building in Coot[49] and restrained refinement in PHENIX[50] were performed, and the simulated annealing protocol was used to reduce potential model bias and generate omit maps. The models were further refined using BUSTER (http://www.globalphasing.com/buster/), and model building was aided by the output of the MolProbity structure validation server[51]. The final refinement protocols included positional, individual B-factor and TLS refinement in all cases. The structures of the complexes S2-HLA-DQ2.5-glia-α1a, S16-HLA-DQ2.5-glia-α2 and D2-HLA-DQ2.5-glia-α2 each contained two protomers per asymmetric unit, and therefore NCS restraints were used throughout refinement. The TCR variable domains were numbered according to the IMGT unique numbering system[52], with the exception of CDR3α in the S2 TCR, where the suffix numbers 0.1 and 0.2 were substituted with the letters .a and .b, respectively. All crystallographic figures were generated in PyMOL (http://www.pymol.org/), and the programs Areaimol and Contacts from the CCP4 program suite[46] were used for BSA and interface contact analysis, respectively. Data processing and refinement statistics are summarized in **Supplementary Table 1**. Ramachandran statistics of the final models indicated that 95–96% of residues had a favored geometry, and the models of S2-HLA-DQ2.5-glia-α1a, S16-HLA-DQ2.5-glia-α2, D2-HLA-DQ2.5-glia-α2 and JR5.1-HLA-DQ2.5-glia-α2 contained 0.45%, 0.13%, 0.58% and 0.39% of Ramachandran outliers, respectively. In the final electron density maps, the HLA-DQ2 antigen binding cleft, antigenic peptides and CDR loops all appeared to be well ordered in all four structures (**Supplementary Fig. 1**).

Surface plasmon resonance measurement and analysis. Equilibrium affinity constants of the TCRs for HLA-DQ2.5-glia-α1a and HLA-DQ2.5-glia-α2 were determined by surface plasmon resonance similarly to previous measurements[25,53]. Briefly, biotinylated HLA-DQ2.5-glia-α1a and HLA-DQ2.5-glia-α2 were immobilized on different streptavidin-coated flow-cell surfaces of a Biacore CAPture sensor chip (1,000–1,400 response units), and an untreated flow cell was used for background correction. After injection of 1 mM biotin, equilibrium affinities were determined in HBS buffer (10 mM HEPES-HCl, pH 7.4, 150 mM NaCl, 0.5 mM EDTA and 0.005% surfactant P20 supplied by the manufacturer) at 20 °C using a Biacore 3000 instrument. Decreasing concentrations of each TCR were passed over the flow cells at 10 µl/min for 2 min. The maximum concentration for all dilution series was in the range of 170–210 µM, with the exception of the S2 TCR, for which a maximum concentration of 82 µM was used because of low protein yields. The equilibrium dissociation constant, K_d, was subsequently obtained by fitting a single-ligand binding model with K_d as a shared parameter to the combined data from different experiments using SigmaPlot (Systat Software).

42. Brochet, X., Lefranc, M.P. & Giudicelli, V. IMGT/V-QUEST: the highly customized and integrated system for IG and TR standardized V-J and V-D-J sequence analysis. *Nucleic Acids Res.* **36**, W503–W508 (2008).
43. Wang, G.C., Dash, P., McCullers, J.A., Doherty, P.C. & Thomas, P.G. T cell receptor αβ diversity inversely correlates with pathogen-specific antibody levels in human cytomegalovirus infection. *Sci. Transl. Med.* **4**, 128ra42 (2012).
44. Clements, C.S. *et al.* The production, purification and crystallisation of a soluble, heterodimeric form of a highly selected T-cell receptor in its unliganded and liganded state. *Acta Crystallogr. D Biol. Crystallogr.* **58**, 2131–2134 (2002).
45. McPhillips, T.M. *et al.* Blu-Ice and the Distributed Control System: software for data acquisition and instrument control at macromolecular crystallography beamlines. *J. Synchrotron Radiat.* **9**, 401–406 (2002).
46. Winn, M.D. *et al.* Overview of the CCP4 suite and current developments. *Acta Crystallogr. D Biol. Crystallogr.* **67**, 235–242 (2011).
47. Kabsch, W. Xds. *Acta Crystallogr. D Biol. Crystallogr.* **66**, 125–132 (2010).
48. Storoni, L.C., McCoy, A.J. & Read, R.J. Likelihood-enhanced fast rotation functions. *Acta Crystallogr. D Biol. Crystallogr.* **60**, 432–438 (2004).
49. Emsley, P. & Cowtan, K. Coot: model-building tools for molecular graphics. *Acta Crystallogr. D Biol. Crystallogr.* **60**, 2126–2132 (2004).
50. Adams, P.D. *et al.* PHENIX: a comprehensive Python-based system for macromolecular structure solution. *Acta Crystallogr. D Biol. Crystallogr.* **66**, 213–221 (2010).
51. Chen, V.B. *et al.* MolProbity: all-atom structure validation for macromolecular crystallography. *Acta Crystallogr. D Biol. Crystallogr.* **66**, 12–21 (2010).
52. Lefranc, M.-P. *et al.* IMGT, the international ImMunoGeneTics information system(R). *Nucleic Acids Res.* **33**, D593–D597 (2005).
53. Liu, Y.C. *et al.* The energetic basis underpinning T-cell receptor recognition of a super-bulged peptide bound to a major histocompatibility complex class I molecule. *J. Biol. Chem.* **287**, 12267–12276 (2012).

doi:10.1038/nsmb.2817